PR6 Improvement of Characterization Techinques in High-Energy-Particle Irradiation Research

A. Kinomura

Institute for Integrated Radiation and Nuclear Science, Kyoto University

OBJECTIVES: Irradiation facilities of high-energy particles for neutrons (Material Controlled irradiation Facility), ions (e.g., Heavy ion irradiation facility) and electrons (Temperature-controlled irradiation facilities, KUR-LINAC) have been extensively developed at the Institute for Integrated Radiation and Nuclear Science. The developed facilities have been in operation and opened for joint research projects. One of the objectives of this project is to further improve or optimize irradia- tion facilities for advanced irradiation experiments.

As characterization techniques for irradiated materials, a slow positron-beam system and a focused ion beam system have been developed and introduced, respectively, in addition to previous characterization facilities such as an electron microscope, an electron-spin-resonance spectrometer, a bulk positron annihilation spectrometer and a thermal desorption spectrometer. Another objective is to introduce new techniques or reconsider analytical methods of previously used characterization techniques.

Based on these two objectives, we expect the enhancement of previous studies and the attraction of new users for the joint research program.

The allotted research subject (ARS) and individual co-researchers are listed below.

ARS-1:
Study on Efficient Use of Positron Moderation Materials (A. Kinomura *et al.*)

ARS-2:
Electron-irradiation effects on diffusion coefficient of Cu in Fe studied by three dimensional atom probe (K. Inoue *et al.*)

ARS-3:
Change in Positron Annihilation Lifetime of Vacancies by Hydrogen Charging in Tungsten (K. Sato *et al.*)

ARS-4:
Gamma-ray irradiation effect on ZnO bulk single crystal (K. Kuriyama *et al.*)

ARS-5:
Establishment of technique for thermal diffusivity measurement using TEM disk size miniature test specimens for post-irradiation experiments (M. Akiyoshi *et al.*)

ARS-6:
Positron Annihilation Study of Fe-Cr binary alloy after Electron Irradiation (T. Onitsuka *et al.*)

ARS-7:
Study on Free Volume in Diamond-like Carbon Thin Films by Positron Annihilation Spectroscopy (K. Kanda *et al.*)

ARS-8
Thermal stability of diamond-like carbon films (S. Nakao *et al.*)

RESULTS: In ARS-1, the performance of the bright- ness enhancement system of the slow positron-beam sys- tem of Kyoto University research Reactor (KUR) was evaluated by using a positron beam as the KUR operation was approved and restarted.

In ARS-2, electron-irradiation for Fe-1.0wt.%Cu alloy was performed with energy of 8 MeV at KUR LINAC. The irradiation temperature was about 750 K.

In ARS-3, high purity tungsten irradiated by 8 MeV electrons were characterized by positron lifetime spectroscopy. After hydrogen charging, the second lifetime decreased because the single vacancies are decorated with hydrogen.

In ARS-4, green luminescence of ZnO after Co-60 gamma-ray irradiation increased by about 14% compared with that of unirradiated ZnO, suggesting that oxygen vacancy and zinc vacancies were introduced by Compton scattering during gamma-ray irradiation.

In ARS-5, the miniature specimen for measurement of thermal diffusivity was validated and this result will be widely used in future materials irradiation studies.

In ARS-6, Fe-40Cr alloy samples after electron irradiation by KURRI-LINAC were characterized by positron annihilation spectroscopy. The result indicated that the rapid increase in the W-parameter due to irradiation.

In ARS-7, positron annihilation measurement was performed at the slow positron beam system (B-1) for three types of DLC (diamond-like carbon) films. The result of S parameters can be considered that hydrogen atoms narrow the free volume in the DLC film.

In ARS-8, the TDS (thermal desorption spectroscopy) measurement at high temperature up to 800 °C was carried out for various DLC and carbon films. There is a possibility that the structural changes may be driven by the creation and annihilation of vacancy and defects caused by hydrogen desorption.

SUMMARY: In addition to developments on the slow positron beamline and a sample holder for electron irradiation, combinations of new materials and different irradiation/characterization techniques were continued. These studies were performed in the line of the objectives of this project. Further studies are in progress for the following year.

PR6-1 Study on Efficient Use of Positron Moderation Materials

A. Kinomura, N. Oshima[1], Y. Kuzuya and A. Yabuuchi

Institute for Integrated Radiation and Nuclear Science, Kyoto University
[1]National Institute of Advanced Industrial Science and Technology (AIST)

INTRODUCTION: Positron annihilation spectroscopy is a unique analytical method to detect vacancies, voids and free volume of materials. Energy-variable mono-energetic positron beams (slow positron beams) are important to perform depth-dependent positron annihilation spectroscopy of thin films or surface layers. Intense positron sources are required to efficiently obtain slow positron beams. Positron sources based on pair creation have higher intensity than radioisotope-based positron sources. Therefore, positron sources using pair-creation by gamma-rays from a nuclear reactor have been developed by using Kyoto University research Reactor (KUR). In the case of the KUR, the source size of the KUR slow positron beam is approximately 30 mm in diameter. For typical sample sizes of materials analysis ($\leq$10 mm), it is necessary to reduce beam sizes efficiently while keeping beam intensity as high as possible. For this purpose, brightness enhancement techniques are used. In this study, we have evaluated the brightness enhancement system in the KUR slow positron beam system.

EXPERIMENTS: The brightness enhancement system of the KUR slow positron beam system has been examined using electron beams after the system was installed [1], since the KUR was not in operation for about 3 years to comply with a new safety criteria. As the KUR operation was restarted on August 2017, the brightness enhancement system was accordingly evaluated by a reactor-based positron beam.

Three types of experiments were performed for the brightness enhancement system: (1) Optimization of bias-voltages and solenoid/Helmholtz coil currents to maximize positron-beam intensities. (2) Examination of focusing performance of the brightness enhancement system. (3) Efficiency evaluation of remoderator thin films.

RESULTS: The positron source of the KUR slow positron beamline consists of a W convertor, two W moderator and extraction electrode, where bias voltages can be applied to each part. Slow positrons generated at the source was transported by magnetic fields formed by solenoid or Helmholtz coils along the beamline to the brightness enhancement system and a sample chamber. Several steering coils were attached to the beamline to optimize beam trajectories. The best combination of voltages for the source components and currents for solenoid, Helmholtz and steering coils was determined by observing the phosphor-screen images and intensities of annihilation gamma-rays on the microchannel plates (MCP's) as shown in Fig. 1. Note that the MCP2 is positioned at the focal point of the lens in the brightness enhancement system. After the optimization, the positron intensity at the sample chamber was measured to be 2.4 $\times 10^6$ e^+/s for the 5 MW operation.

Spot sizes of the positron beam were measured from pictures of the MCP phosphor screens before and after the brightness enhancement. Spot sizes for horizontal and vertical directions were slightly different. A spot area was reduced by a factor of ~20 after focusing at the brightness enhancement system.

Remoderation efficiencies were evaluated from annihilation gamma-ray intensities by comparing MCP1 and MCP3 in Fig. 1. Fig. 2 shows the typical gamma-ray spectra measured by a Ge detector. Gamma-ray intensities were calculated after the subtraction of background gamma-rays without introducing the positron beam. The efficiency was measured to be ~2%.

In summary, the brightness enhancement system of the KUR slow positron system was evaluated with a positron beam during the KUR operation. Demagnification factors and remoderation efficiencies were successfully measured. We plan further optimization of the system in the near future.

REFERENCE:

[1] Y. Kuzuya et al. J. Phys. Conf. Series 791 (2017) 012012.

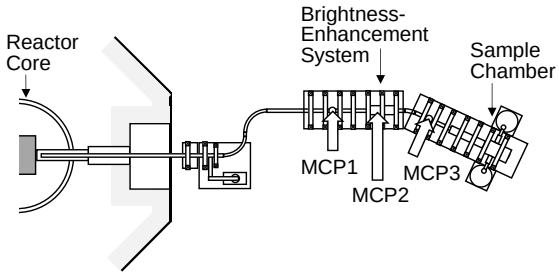

Fig. 1. Schematic view of the beamline and the positions of the brightness enhancement system and microchannel plates (MCP1, MCP2 and MCP3).

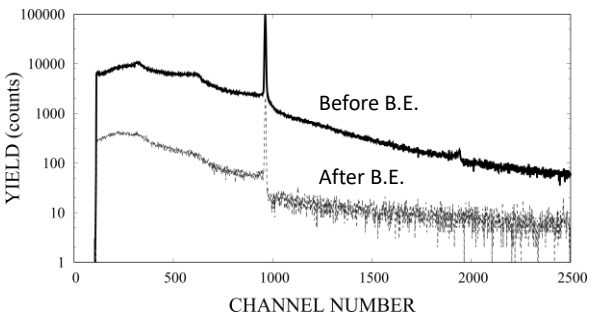

Fig. 2. Gamma-ray spectra before and after brightness enhancement (B.E.).

PR6-2 Electron-Irradiation Effects on Diffusion Coefficient of Cu in Fe Studied by Three Dimensional Atom Probe

T. Toyama, K. Inoue, Y. Nagai, Y. Shimizu,
M. Shimodaira, Y. Tu, C. Zhao, T. Onitsuka[1],
A. Kimomura[2], T. Yoshiie[2], Q. Xu[2] and A. Yabuuchi[2]

Institute for Materials Research, Tohoku University
[1]Research Institute of Nuclear Engineering, Fukui University
[2]Research Reactor Institute, Kyoto University

INTRODUCTION: Reactor pressure vessel (RPV) is one of the most important parts in nuclear power plant since RPV holds nuclear fuels, control rods and primary cooling water. Therefore, irradiation-induced embrittlement of RPV steels is vital issue for the safe operation of nuclear power plants. Substantial studies have revealed that nano-sized Cu precipitates are formed by neutron-irradiation and cause the embrittlement. In order to understand the kinetics of Cu precipitation, the diffusion coefficient, *D*, of Cu in Fe is the important basic quantities [1, 2].

It is predicted that diffusivity of Cu may be strongly affected by irradiation [3]; for example, diffusivity is greatly enhanced by irradiation because vacancies and interstitials, which are necessary for diffusion of solute atoms, are remarkably induced during irradiation. Such enhancement of diffusion has been modeled and simulated, however, experimental studies are very limited at present. We employ KUR LINAC to induce simple Frenkel pairs, and investigate the electron-irradiation effects on Cu diffusivity in Fe. In the previous report, we studied Cu diffusivity by using conventional Cu-Fe diffusion couples but the irradiation-effects was not very clear probably due to the detection limitation of three-dimensional atom probe (3D-AP). In this study, Fe-1.0wt.%Cu alloy is electron-irradiated at KUR LINAC to investigate the *D* of Cu in Fe via the kinetics of Cu precipitation.

EXPERIMENTS: Fe-1.0wt.%Cu alloy was made from high-purity (5N) Fe and Cu. A plate of 5 mm × 5 mm × 1 mm was fabricated and the surface of the sample was mechanically polished with abrasive papers of #2000. After removal of the machined layer by chemical polishing, the sample was annealed at 1100K for 4 hours followed by quenching into ice-water.

Electron-irradiation was performed with electron beam with energy of 8 MeV at KUR LINAC. The irradiation temperature and the irradiation time were about 750 K and 30000 seconds, respectively.

After electron-irradiation, needle-like samples for 3D-AP were fabricated with focused-ion beam apparatus. In 3D-AP measurement, a voltage pulse mode was employed at temperature of 50 K, pulse fraction of 20%, and a repetition frequency of 200 kHz.

RESULTS: Figure 1 shows atom map of Cu in the electron-irradiated Fe-Cu alloy. 3D-AP measurements were performed for several needle-like samples, and the similar results to fig. 1 were obtained. Cu precipitates were clearly observed and the number density and the average size of Cu precipitates were analyzed with the standard analysis method. The Cu concentration in Fe matrix was also analyzed. With these parameters, the diffusion coefficient of Cu was estimated by using a formula concerning the diffusion coefficient and precipitation kinetics [4]. Figure 2 shows the Arrhenius plot of the *D* of Cu in Fe in the studied sample together with the *D* under thermal-aged samples [1]. The *D* obtained in this study was 9~23 times higher than that in thermal-aged condition, clearly indicating that the Cu diffusivity is enhanced by electron-irradiation. In future work, the Fe-Cu alloys will be irradiated at the temperature other than 750K to reveal the temperature dependency of *D* for further understanding of the electron-irradiation effects on *D*.

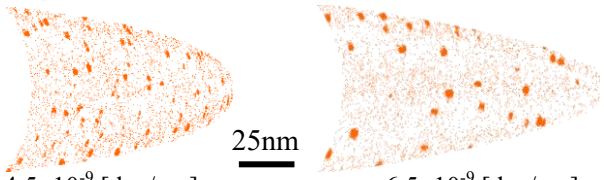

Figure 1: Atom maps of Cu in the electron-irradiated Fe-1.0wt. %Cu alloy.

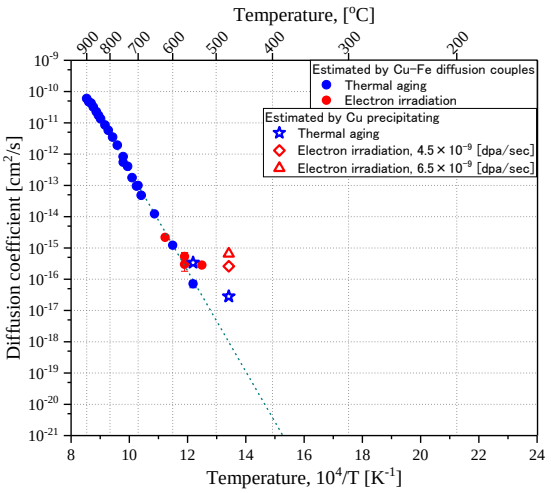

Figure 2: Arrhenius plot of the diffusion coefficient of Cu in Fe.

REFERENCES:

[1] T. Toyama *et al.*, Scrip. Mater., **83** (2014) 5-8.
[2] M. Shimodaira *et al.*, Mater. Trans., **9** (2015) 1513-1516.
[3] R. Sitmann, J. Nucl. Mater., **69&70** (1968) 386-412.
[4] For example, M. Koiwa and H. Nakajima, Diffusion in materials (Uchidarokakuho, 2009).

PR6-3 Change in Positron Annihilation Lifetime of Vacancies by Hydrogen Charging in Tungsten

K. Sato, A. Hirosako, K. Ishibashi[1], Y. Miura, Q. Xu[1], A. Kinomura[1], T. Yoshiie[1]

Graduate School of Science and Engineering, Kagoshima University
[1]Research Reactor Institute, Kyoto University

INTRODUCTION: The study of defect-hydrogen isotope complexes is an important issue for the structural materials of fusion reactor. In fusion reactor, neutrons introduce not only a variety of defects but also hydrogen and helium atoms formed by nuclear reaction of (n,p) and (n,α), respectively. In plasma-facing materials (PFMs), hydrogen isotopes penetrate by exposure to fusion plasma. The hydrogen isotopes interact with the irradiation-induced defects, and remain in the materials [1−3]. Retention of hydrogen isotopes leads to a decrease in mechanical properties of materials, e.g. hydrogen embrittlement etc. Tungsten is one of strong candidates for PFMs, which have high melting point, high thermal conductivity, and low sputtering erosion. However, hydrogen solubility is quite low, and interaction between hydrogen atoms and defects is strong [4]. Therefore, to study the interaction between hydrogen and defects is especially important in tungsten. In this study, we estimate the number of hydrogen trapped at single vacancies by the following procedures. (1) Vacancies are introduced to re-crystallized tungsten by electron irradiation. (2) Hydrogens are charged to the electron-irradiated samples. (3) The change in positron annihilation lifetime (PAL) by hydrogen charging is detected. (4) PAL is simulated using the exact structure obtained by the first principle calculation. (Hydrogens are put on the inner surface of vacancies.) (5) Results between experiments and simulations are compared.

EXPERIMENTS: High purity tungsten (99.95%, A.L.M.T. Corp.) samples were used in this study. Samples with diameters of 5 mm were cut by wire electric discharge machine from 0.2 mm thick sheets and annealed at 1773 K for 1 h in a vacuum (< 10^{-4} Pa) for re-crystallization. Defects were introduced by irradiation with electrons at 8 MeV using the Electron Linear Accelerator of the Research Reactor Institute, Kyoto University. The irradiation doses were 1.4×10^{22}, 3.0×10^{22}, and 6.6×10^{22} /m^2 (1.4×10^{-4}, 2.9×10^{-4}, 6.4×10^{-4} dpa). For dose calculations, we used the atomic displacement cross section of 70.4 barns and the displacement threshold energy of 84 eV [5]. The irradiation temperature was kept at 363 ± 10 K by water cooling. All samples were electropolished after electron irradiation to remove oxidation layers formed by water cooling. High pressure hydrogen charging (H.C.) was employed in this study. Pressure, temperature, and time for H.C. was 5.8 MPa, 573 K, and 240 h, respectively. Before H.C., electron-irradiated samples were annealed at 573 K for 240 h (same condition as the H.C.) in a vacuum to avoid the formation of vacancy clusters during H.C. The PAL measurements were performed at room temperature. The system used in this study was a fast-fast coincidence system with a time resolution of 190 ps (full width at half maximum; FWHM). The PAL spectra were accumulated with a total count of approximately 3×10^6 and were analyzed using the PALSfit package [6].

RESULTS: In tungsten irradiated with electrons at doses of 6.4×10^{-4} dpa, before annealing at 573 K for 240 h, small interstitial clusters are formed by electron irradiation, and positrons are annihilated at not only vacancies but also small interstitial clusters, however, during annealing, interstitial clusters are annihilated at sinks or grow. Therefore, although the PAL spectrum could not be decomposed into two components after electron irradiation, we could accomplish it after annealing. From the PAL of approximately 175 ps after annealing, vacancy clusters are not formed by annealing. After H.C., τ_2 decreases because the single vacancies are decorated with hydrogen. Until the isochronal annealing at 523 K, τ_1, τ_2, τ_m, and I_2 are almost constant. After annealing at 573 K for 1 h, τ_1, τ_2, and τ_m increase and I_2 decreases, which denotes the formation of vacancy clusters. When the annealing time at 573 K increases, τ_2 increases further. This means the growth of vacancy clusters.

The change in the PAL at doses of 2.9×10^{-4} dpa before and after annealing at 573 K for 240 h is also caused by the annihilation or growth of interstitial clusters. Trend of the change in the PAL is almost the same as that of the sample at doses of 6.4×10^{-4} dpa. In the annealing at 573 K for 10 h, the PAL starts to increase. I_2 is almost constant until the annealing at 573 K for 20 h. These are different from that of the sample at doses of 6.4×10^{-4} dpa. Therefore, this increase of the PAL in the annealing at 573 K for 10 h is due to the dissociation of hydrogen atoms from vacancies. After annealing at 573 K for 44 h, I_2 decreases and τ_2 gradually increases with increasing the annealing time. This indicates the formation of vacancy clusters. Kato *et al*. reported that hydrogen assisted the formation of di-vacancies (hydrogen-di-vacancy complexes were very stable) [7]. This mechanism may make the formation of vacancy clusters easy in this study. When samples did not contain hydrogen, Sato et al. did not detect the formation of vacancy clusters in tungsten irradiated with electrons at doses of 3.2×10^{-5} dpa by the isochronal annealing [5].

REFERENCES:

[1] N. Yoshida, J. Nucl. Mater., **266-269** (1999) 197.
[2] M. Tokitani *et al.*, J. Nucl. Mater., **363** (2007) 443.
[3] V.Kh. Alimov *et al.*, J. Nucl. Mater., **375** (2008) 192.
[4] K. Ohsawa *et al.*, Phys. Rev., B **82** (2010) 184117.
[5] K. Sato *et al.*, Nucl. Mater. Ene., **9** (2016) 554.
[6] J.V. Olsen *et al.*, Phys. Stat. Sol., C **4** (2007) 4004.
[7] D. Kato *et al.*, J. Nucl. Mater., **417** (2011) 1115.

PR6-4 Gamma-ray Irradiation Effect on ZnO Bulk Single Crystal

K. Kuriyama, Y. Torita, K. Sato, J. Tashiro, K. Kushida[1], A. Yabuuchi[2], Q. Xu[2] and A. Kinomura[2]

College of Engineering and Research Center of Ion Beam Technology, Hosei University
[1]Osaka Kyoiku University
[2]Research Reactor Institute, Kyoto University

INTRODUCTION: Examining the defects caused by various radiations to ZnO and GaN by assuming the space environment is important. In our previous study, we reported the modification of the yellow luminescence in GaN bulk single crystal by gamma-ray irradiation [1]. The resistivity varies from 30 Ωcm for an un-irradiated sample to 10^4 Ωcm for gamma-ray irradiated one. The high resistivity was attributed to the carrier compensation due to the deep acceptor level relating to interstitial nitrogen atoms. We also reported that the persistent photoconductivity by electron-irradiated ZnO [2] and a shallow donor level relating to hydrogen interstitial by H-ion implanted ZnO [3]. In the present study, we report the green luminescence (GL) in ZnO bulk single crystals caused by gamma-ray irradiation.

EXPERIMENTS: ZnO bulk single crystals with a thickness of 500 μm were used. The crystals were irradiated at room temperature with gamma-rays of 1.17 and 1.33 MeV from a cobalt-60 source of Kyoto University Research Reactor Institute. Samples were irradiated with an absorption dose rate of 1.771 KGy/h. Total gamma-ray dose was 170 kGy. The resistivity varied from 4.1 x 10^4 Ωcm for an un-irradiated sample to 3.1 x 10^2 Ωcm for gamma-ray irradiated one. Photoluminescence (PL) spectra were measured at 16 K using a He-Cd laser.

RESULTS: The band edge emission was observed at 275 nm in both un-irradiated and gamma-ray irradiated samples. The GL from the un-irradiated ZnO with a peak at 535 nm (2.31 eV) was observed at around 430 nm to 670 nm, whereas the GL intensity of the gamma-ray irradiated ZnO increased to about 14 % in comparison with that of un-irradiated ones, suggesting that oxygen vacancy (V_O) and zinc vacancy (V_{Zn}) were induced by Compton electrons emitted by the gamma-ray irradiation. This PL peak is a superposition consisting of the ~490 nm-emission relating to the V_{Zn} and ~530 nm -emission relating to V_O. The PL intensity of V_O is eight times larger than that of V_{Zn}. The existence of V_{Zn} would suggest the formation of zinc interstitial (Zn_i). In analogy with the low resistivity after Al-implanted ZnO [4], the origin of the low resistivity in gamma-ray irradiated ZnO would be attributed to the Zn_i located at ~30 meV below the conduction band [5].

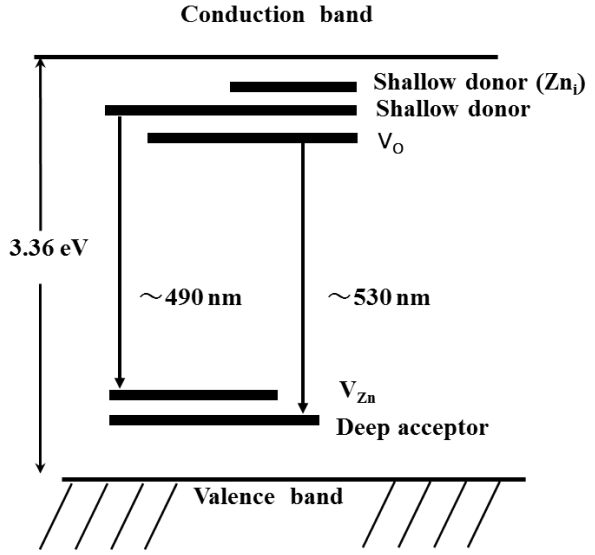

Fig.1 Schematic energy level of the green luminescence in gamma-ray irradiated ZnO. The gamma-ray induced shallow donor relating to zinc interstitial (Zn_i) is located at about 30 meV below the conduction band.

REFERENCES:

[1] Y. Torita, N. Nishikata, K. Kuriyama, K. Kushida, A. Kinomura, and Q. Xu, Proceedings of ICPS2016 (Journal of Physics, IOP(UK)) **864**, 012016 (2017).
[2] T. Oga, Y. Izawa, K. Kuriyama, K. Kushida, and Q. Xu, Solid State Commun., **151** (2011) 1700.
[3] T. Kaida, K. Kamioka, T. Ida, K. Kuriyama, K. Kushida, and A. Kinomura, Nucl. Instrum, Method Phys. Res. B, **332** (2014) 15.
[4] T. Oga, Y. Izawa, K. Kuriyama, K. Kushida, and A. Kinomura, J. Appl. Phys., **109** (2011)123702.
[5] D. C. Look, J. W. Hemsky, and J. R. Sizelove, Phys. Rev. Lett., **82** (1999) 2552.

PR6-5 Establishment of Technique for Thermal Diffusivity Measurement using TEM Disk Size Miniature Test Specimens for Post-irradiation Experiments

M. Akiyoshi, M. Yashiki[1] and A. Kinomura[2]

Radiation Research Center, Osaka Prefecture University
[1]Grad. School of Eng., Osaka Prefecture University
[2]Research Reactor Institute, Kyoto University

INTRODUCTION:

Radioactivity levels for conventional thermal diffusivity test specimens are often prohibitively high for examination with candidate metallic materials, such as tungsten and reduced activation steels for fusion energy. Therefore, in the ongoing Japan-US PHENIX project, irradiation in the High Flux Isotope Reactor (HFIR) was performed with the miniature specimen form of diameter (D) 3mm×thickness (T) 1/2 mm small disk for thermal diffusivity measurement. In this study, the thermal diffusivity measurement of this D3TH miniature specimen is validated using a Netzsch LFA-467 `Hyper Flash' thermal analyzer and `Graphene Nanoplatelets containing agent'. With careful surface treatment and data analysis, the D3TH specimens showed almost the same value as the diameter 10mm×thickness 2mm (D10T2) standard specimens.

EXPERIMENTS and RESULTS:

Using the conventional Netzsch LFA-457 thermal analyzer, a D3TH specimen was measured to verify the influence of thickness. With this system, the pulse-width of the laser flash is not fast enough to measure a tungsten specimen of 0.5mm thickness correctly, and consequently, the result showed large difference between D10T2 standard specimen and D3TH miniature specimens. Then, using a new Netzsch LFA-467 `Hyper Flash' thermal analyzer, a D10TH specimen was measured to verify the influence of thickness. In this system, the pulse-width of laser flash is enough fast to measure β-SiC specimens of 0.5mm thickness correctly.

However, the first measurement showed a large disagreement from the standard specimen, which was considered to be caused by the surface treatment. Netzsch resolved this problem with the surface treatment `Graphene Nanoplatelets containing agent'[1] that can be applied as a very thin coating. Fig. 1 shows a very thin, sparse coated surface. Even such a thin coating on a polished tungsten specimen enabled the thermal diffusivity to be measured correctly. Finally, using the Netzsch LFA-467 with the Graphene agent, D3TH specimens were evaluated successfully at a room temperature and a tungsten specimen was measured at elevated temperature. Fig. 2 shows the thermal diffusivity of the tungsten specimens at elevated temperature. In this figure, the D3TH specimen shows almost same thermal diffusivity especially at higher temperatures. The obtained α(300) from the fitting curve for D10T1 standard specimen was 66.6mm^2/s, and for D3TH 68.2mm^2/s that is only 2.3% higher than the standard specimen. This difference is small enough for the continued use of the D3TH specimen size for the actual application.

CONCLUSION:

It is concluded that the miniature specimen for measurement of thermal diffusivity is validated and this result will be widely used in future materials irradiation studies. This result is already reported at ISFNT-13 and published in Fusion Engineering and Design[2].

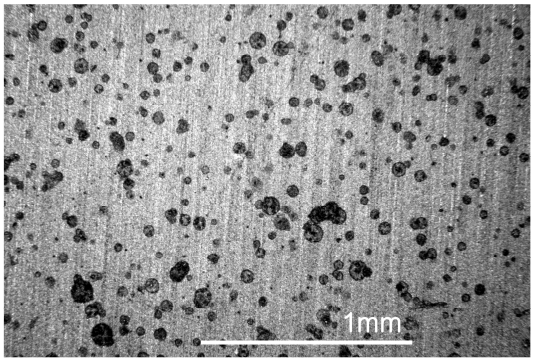

Fig.1 Sparsely coated surface of a specimen using a 'graphene nanoplatelets containing agent'.

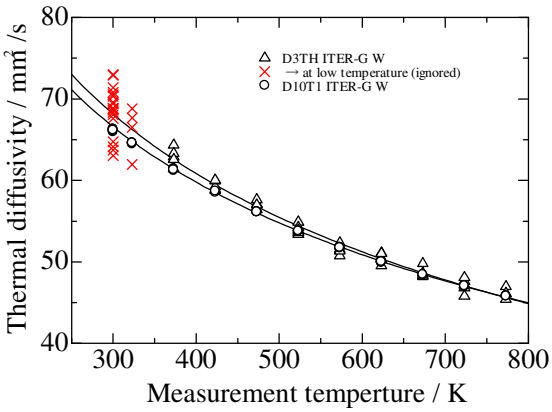

Fig. 2 Validation of thermal diffusivity measurement using D3TH (diameter 3mm × thickness 0.5 mm) tungsten specimen using Netzsch LFA-467 and graphene agent

REFERENCES:

[1] Y. Ishibashi *et al.*, The 37th Japan Symposium on Thermophysical Properties, Nov.28-30, 2016, Okayama.
[2] M. Akiyoshi, R. Kasada, Y. Ishibashi, L.M. Garrison, J.W. Geringer, W.D. Porter and Y. Katoh, Validation of miniature test specimens for post-irradiation thermal diffusivity measurement, Fusion Engineering and Design (in press, https://doi.org/10.1016/j.fusengdes.2018.03.008)

PR6-6 Positron Annihilation Study of Fe-Cr binary alloy after Electron Irradiation

T. Onitsuka, K. Sato[1] and Q. Xu[2], A. Kinomura[2], A. Yabuuchi[2] and K. Fukumoto

Research Institute of Nuclear Engineering, Fukui University
[1]Graduate School of Science and Engineering, Kagoshima University
[2]Institute for Integrated Radiation and Nuclear Science, Kyoto University

INTRODUCTION: High-chromium (9-12%Cr) Ferritic/martensitic steels are attractive candidate material for various nuclear energy systems. The phase decomposition into the Fe-rich and the Cr-rich phases are the main reason for the so-called 475 ℃ embrittlement that may occur in technologically important structural materials made on the base of Fe-Cr alloys such as High-chromium steels, if subjected to temperatures between 300 and 600 ℃ [1]. This phase decomposition and irradiation induced degradation are expected to be the critical issues for reactor operation. The purpose of this study is to examine the effect of thermal aging and the irradiation on the phase decomposition of the high-chromium Ferritic/martensitic steels. In the previous study, we authors have reported on the result of electron irradiation experiment at 100 ℃. In this paper, we report on the result of the electron irradiation experiment at 475 ℃.

EXPERIMENTS: Simple binary Fe-40Cr model alloy was made by arc melting under argon atmosphere in a water-cooled copper hearth. All the ingots were melted and inverted three times in order to promote chemical homogeneities. The obtained ingot was conducted by solution heat treatment at 850 ℃ for 2 h followed by water quenching, and then, machined to the dimensions of 10 mm × 10 mm × 0.5mm. The electron irradiation at 475 ℃ in the helium atmosphere, was performed up to 0.33×10^{-3} dpa via the 8 MeV KURRI-LINAC. After the irradiation, all specimens were mechanically polished and then electrolytically polished to clean the surface. Finally microstructural characterization was performed by positron annihilation lifetime measurement and Coincidence Doppler Broadening (CDB) of positron annihilation radiation measurement to examine the microstructural change in atomic level during irradiation and thermal aging process.

RESULTS: Table. 1 shows the result of positron lifetime measurement in irradiated and unirradiated Fe-40Cr, and pure bulk materials (Fe and Cr). Only one lifetime component was found in the irradiated specimens as well as the unirradiated specimens. The lifetime for the irradiated specimens around 107 psec are very close to the lifetime in the unirradiated specimens. This shows that there is no vacancy-type defects could be found after irradiation. Based on previous studies, it is believed that small vacancy clusters become thermally unstable at higher temperature such like 475 ℃ and more likely to dissociate into single vacancies which can move immediately and then disappear on various sinks such as free surfaces, grain boundaries. Fig.1 shows the S-W plots obtained from the CDB measurements in the Fe-40Cr alloy before (as W.Q.) and after the irradiation. In general, when the positron is trapped in vacancy-type defect, the S-parameter increases but the W-parameter decreases. On the other hand, when the Fe/Cr phase decomposition occurred, the W-parameter increases but the S-parameter decreases. The result indicated that the rapid increase in the W-parameter due to irradiation. Thus, it might be inferred from these results that the early stage of phase decomposition was detected in the irradiated specimens. Further studies and experiments are necessary in order to make it clear the difference between the aging effect and the irradiation effect.

REFERENCE:

[1] K. Okano *et al.*, Nucl. Instr**.** and Meth., **186** (1981) 115-120.

Table. 1. Measured positron lifetimes in the irradiated and unirradiated specimens.

Specimen	dpa (10^{-3})	Irradiation Temp. (℃)	Irradiation Time (h)	Positron lifetime (psec)
Fe (bulk)	-	-	-	105.4
Cr (bulk)	-	-	-	105.6
Fe-40Cr	-	-	-	107.5
Fe-40Cr	0.03	475	2	107.3
Fe-40Cr	0.33	475	20	107.1

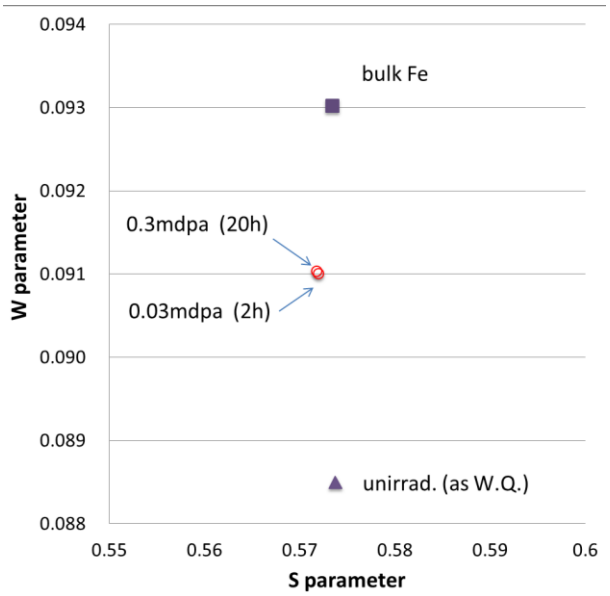

Fig. 1. Plot of the S-W values of the irradiated specimens. Unirradiated Fe-40Cr (W.Q) and pure bulk Fe are also plotted.

PR6-7 Study on Free Volume in Diamond-like Carbon Thin Films by Positron Annihilation Spectroscopy

K. Kanda, F. Hori[1], A. Yabuuchi[2] and A. Kinomura[2]

Laboratory of Advanced Science and Technology for Industry, University of Hyogo
[1]Department of Materials Science, Osaka Prefecture University
[2]Institute for Integrated Radiation and Nuclear Science, Kyoto University

INTRODUCTION: Amorphous carbon films, which are usually called diamond-like carbon (DLC) films, have attracted considerable attention in recent years for many reasons, such as excellent corrosion resistance, high hardness, and high wear resistance [1]. The structure of DLC films is complex, being comprised of an amorphous mixture of sp^2 and sp^3 hybridized carbon atoms combined with hydrogen atoms in the local structure [2].The chemical structure in terms of the coordination of carbon (sp^2 and sp^3 hybridization) and hydrogen atoms are the most important factors governing the quality of DLC films and they are used as classification criteria in ISO20523 published in 2017 [3]. However, DLC films have another structural factor, free volume. Free volume was considerable to connect strongly with several important properties of DLC film, such as hardness, Young modulus, and friction coefficient, but it has not been investigated. Positron annihilation spectroscopy (PAS) is a powerful tool for measuring free volume in material. In the present study, several DLC films were analyzed by PAS to evaluate the free volume in DLC films.

EXPERIMENTS: We prepared four kinds of DLC films using different three deposition methods, 1) filtered cathodic vacuum arc (FCVA) method, 2) ion plating (IP) method, and 3) plasma enhanced chemical vapor deposition (PECVD) method. FCVA DLC film and IP-DLC film were typical DLC film used as hard film, which densities were expected about 2 g/cm^3 and hydrogen contents in these film were expected to lower 20 %. PE-CVD DLC film was highly hydrogenated DLC film, whose hydrogen content was estimated ≈40 % and its density was obtained to 1.25 g/cm^3. Last sample was prepared by the PE-CVD DLC film exposed to synchrotron radiation (SR) at BL06 in the NewSUBARU synchrotron facility of the University of Hyogo [4]. The SR at the BL06 sample stage had a continuous spectrum from the infrared to soft X-ray region and an energy below 1 keV. Every DLC films were deposited onto Si substrate and their film thickness were 100~200 nm.

PAS measurement was performed at the slow positron beam system (B-1). Energy of incident positron, E, ranging 0.5 - 15 keV. Doppler broadening profiles of annihilation γ-rays were obtained using a Ge detector for each positron energy. The-low momentum part of spectra was characterized by the S parameter, which is defined as the number of annihilation events over the range of 511 ± 0.76 keV.

RESULTS: Figure 1 shows the S parameter as a function of incident positron energy E for the FCVA DLC film, IP DLC film, and PECVD DLC film. The S values in the E region lower than 2 keV can be considered to attribute to the annihilation of positrons trapped in free volume in the DLC films. The S values of PECVD DLC film were smaller than those of FCVA DLC film and IP DLC film, in spite of the fact that the density of PECVD DLC film was low. These results can be considered that hydrogen atoms narrow the free volume in the DLC film.

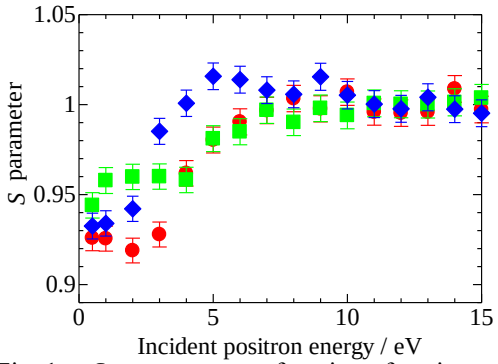

Fig. 1. S parameter as a function of positron energy E for FCVA DLC film ◆, IP DLC film ■, and PECVD DLC film ● .

Figure 2 shows the S parameter for the PECVD DLC film and the PECVD DLC film exposed to SR. The S value of PECVD DLC film was raised by the exposure to SR. This increase was ascribable to the enhancement of free volume in the PECVD DLC film by desorption of hydrogen from film due to excitation of soft X-rays [5].

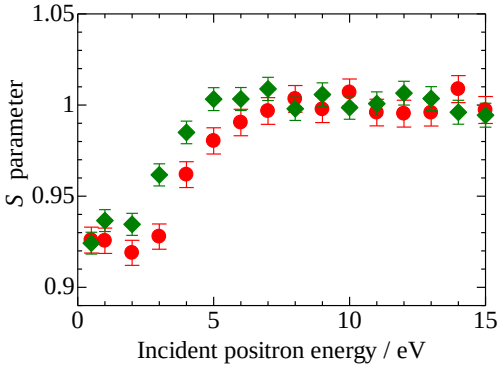

Fig. 2. S parameter as a function of positron energy E for PECVD DLC film ● and that exposed to SR ◆.

REFERENCES:

[1] S. Aisenberg *et al*., J. Appl. Phys., **42** (1971) 3963.
[2] J. Robertson, Surf. Coat. Technol., **50** (1992) 185.
[3] ISO20523, "Carbon based films – Classification and designations".
[4] K. Kanda *et al*., Jpn. J. Appl. Phys., **42** (2003) 3983.
[5] K. Kanda *et al*., Jpn. J. Appl. Phys., **50** (2011) 055801.

PR6-8 **Thermal Stability of Diamond-like Carbon Films**

S. Nakao, X. Qu[1], A. Yabuuchi[1] and A. Kinomura[1]

Structure Materials Research Institute, National Institute of Advanced Industrial Science and Technology
[1]Institute for Integrated Radiation and Nuclear Science, Kyoto University

INTRODUCTION: Diamond-like carbon (DLC) films have attracted much attention because of their excellent mechanical properties, such as high hardness, high wear resistance and low friction coefficients. However, the properties strongly depend on the microstructure of the films which is varied by the deposition conditions and methods. Recently, DLC or carbon films are categorized from type I to VI, which includes graphite-like carbon (GLC) and polymer-like carbon (PLC).
The thermal stability of the films is of importance for practical applications. However, the thermal stability is not always enough to use it at high temperature. It is considered that the changes of the microstructure at high temperature should be responsible for the degradation of the properties. The structural changes are related to H desorption and behavior of defects at high temperature. Many studies have been carried out on the thermal stability of DLC films. However, the principal phenomena, such as defect behavior, are not always clear. Therefore, to make clear the thermal stability of DLC or carbon films, the examination of every type of DLC films (type I to VI) are necessary. The aim of this study is to clarify the relationship between the thermal stability and the behavior of defects and bonded hydrogen in several types of DLC films by positron annihilation and thermal desorption (TDS) method.
In a previous report [1], the films of type I and IV were examined by TDS measurement in the range of room temperature (RT) to 600°C and it was found that hydrogen desorption was clearly observed around 400°C in the case of type IV films. On the other hand, type I films did not change significantly until 600°C. The result suggested that further high temperature was required to characterize all films. In this study, the TDS measurement at further high temperature up to 800°C is carried out together with other types of DLC and carbon films.

EXPERIMENTS: Samples of A – E for TDS measurement are listed in Table 1. Type I (ta-C) and III (a-C) films were prepared by arc ion plating (AIP) at Nippon ITF Inc. and high-power impulse magnetron sputtering (HiPIMS), respectively. Type IV (a-C:H), V (GLC) and VI (PLC) films were deposited by plasma-based ion implantation (PBII) under the different conditions. The details on the PBII system were reported elsewhere [2]. Si wafer was used as substrate. The TDS spectra of Si substrate were also measured for comparison (not shown). The samples were thermally heated from RT to approximately 800°C. The desorption H, H_2, D and DH were detected.

Table 1. Samples for thermal desorption measurement.

Sample	Type	Description	Preparation
A	I	ta−C	AIP
B	III	a−C	HiPIMS
C	IV	a−C:H	PBII
D	V	GLC	PBII
E	VI	PLC	PBII

RESULTS: Figure 1 shows the H_2 desorption spectra of the samples at elevated temperature. The desorption increases with increasing temperature. For the sample A, however, no significant desorption peak of H_2 is observed in this range. The tendency is almost the same as Si substrate. This shows that the sample A is thermally stable up to 800°C. On the other hand, the desorption is gradually increased around 600°C for the samples of B – D. In the case of sample E, the desorption begins to increase around 400°C. These results show that hydrogen is released from the films over 600°C and 400°C for the samples B – D and the sample E, respectively. From the results, it is suggested that thermal stability of sample A is the best among the samples. In addition, the structural changes should begin around 600°C and 400°C due to hydrogen release for the sample B – D and the sample E, respectively. There is a possibility that the structural changes may be driven by the creation and annihilation of vacancy and defects caused by hydrogen desorption. Positron annihilation measurement will be planned next time.

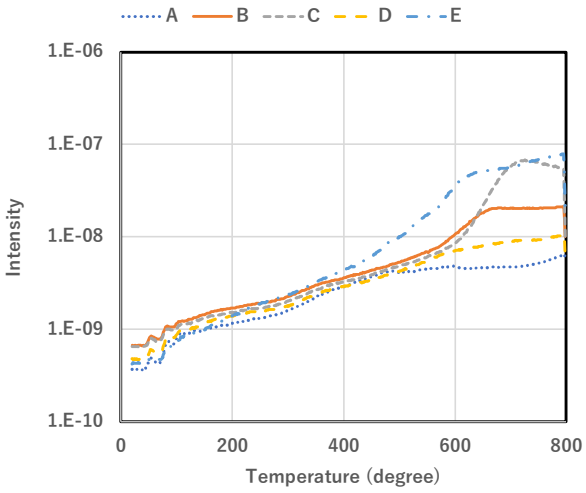

Fig.1 Thermal desorption spectra of H_2 for the samples A – E as a function of elevated temperature. The samples A – E correspond to the films of type I, III, IV, V and VI, respectively.

REFERENCES:
[1] S. Nakao *et al.*, KURRI Progress Report 2016, 28P12-8 (2016) 57.
[2] S. Miyagawa *et al.*, Surf. Coat. Technol., **156** (2002) 322-327.

29P6-8